

Article

Preparation and Characteristics of Corn Straw-Co-AMPS-Co-AA Superabsorbent Hydrogel

Wei-Min Cheng ^{1,*}, Xiang-Ming Hu ^{1,2,*}, De-Ming Wang ³ and Guo-Hua Liu ⁴

Received: 20 September 2015; Accepted: 13 November 2015; Published: 24 November 2015

Academic Editor: Antonio Pizzi

¹ State Key Laboratory Cultivation Base of Mining Disaster Prevention and Control, College of Mining and Safety Engineering, Shandong University of Science and Technology, Qingdao 266590, China

² College of Resources and Environmental Engineering, Binzhou University, Binzhou 256603, China

³ Key Lab of Gas and Fire Control for Coal Mines of Ministry of Education, Faculty of Safety Engineering, China University of Mining and Technology, Xuzhou 221116, China; wdmcumt@163.com

⁴ College of Petrochemical Engineering, Lanzhou University of Technology, Lanzhou 730050, China; 13754689387@163.com

* Correspondence: chengmw@163.com (W.-M.C.); xiangming0727@163.com (X.-M.H.);
Tel.: +86-543-3191-865 (X.-M.H.); Fax: +86-543-3190-000 (X.-M.H.)

† These authors contributed equally to this work.

Abstract: In this study, the corn straw after removing the lignin was grafted with 2-acrylamido-2-methylpropanesulfonic acid (AMPS) to prepare sulfonated cellulose. The grafting copolymerization between the sulfonated cellulose and acrylic acid (AA) was performed using potassium persulfate and *N,N'*-methylenebisacrylamide as the initiator and crosslinking agent, respectively, to prepare corn straw-co-AMPS-co-AA hydrogels. The structure and properties of the resulting hydrogels were characterized by Fourier transform infrared spectroscopy, X-ray diffraction, scanning electron microscopy, thermogravimetric analysis, and dynamic rheometry. The effects of initiator, crosslinker, monomer neutralization degree, and temperature on the swelling ratio of the hydrogels were studied. The water retention, salt resistance, and recyclability of the corn straw-co-AMPS-co-AA hydrogels were also investigated. The optimum water absorptivity of the corn straw hydrogels was obtained at a polymerization temperature of 50 °C with 1.2% crosslinker, 1:7 ratio of the pretreated corn straw and AA, 2% initiator, and 50% neutralized AA.

Keywords: corn straw; sulfonated cellulose; superabsorbent hydrogel; acrylic acid; water absorption

1. Introduction

Superabsorbent hydrogels are a new class of polymeric material with strong hydrophilic groups and can absorb 100–1000 times water of its own weight [1–3]. Owing to their super strong water absorption ability, they have been extensively used in agriculture and forestry, construction, medical [4,5] and public health, and daily life supplies [6–9]. In fact, ~90% of superabsorbent hydrogels are disposable products [10,11], and most of them are synthesized by the graft copolymerization between hydrophilic monomers with double bond such as acrylic acid (AA) and acrylamide (AM). These hydrogels have some drawbacks such as high cost, hard to degrade, and harmful to the environment [12,13]. With deficiency in petroleum products and from the environmental perspective, and cost-effectiveness, superabsorbent hydrogels prepared from natural polyhydroxyl materials have been a hot research field. Natural polyhydroxyl compounds such as starch, cellulose, chitosan, sodium alginate, and humic acid are easy to degrade, prepare, and

recyclable by microbes and plants. Therefore, polyhydroxyl compounds have been widely used to synthesize superabsorbent polymers [2,3,14–16].

Straws are important recyclable resources in nature owing to their extensive source, low cost, biodegradability, and high cellulose content [17]. Recently, using the term “super-absorbent” is preferred, and besides preparing feed and alcohol, a large amount of straw is burned, resulting in waste and environmental pollution [18,19]. Recyclability of waste straws for producing superabsorbent hydrogels after simple pretreatment is not only a beneficial use of the natural resource, but also decreases the cost of hydrogel production, thus overcoming the low efficiency of straw disposal. Moreover, the residual lignin and hemicellulose can be used as fertilizer and promoted in agriculture [20]. In recent years, significant studies have been reported on the synthesis of superabsorbent hydrogels using straws [21–23]. Basta *et al.* [7] graft copolymerized rice straws with sodium acrylate to prepare superabsorbent hydrogels and successfully used them to treat wastewater containing heavy metals. Swantomio *et al.* [24] synthesized rice straw cellulose-acrylamide hydrogels by γ -irradiation. Li *et al.* [21] copolymerized superabsorbent resin by wheat straw, AA, AM, and dimethylhexadiene. Xie *et al.* [20] prepared superabsorbent hydrogels from wheat straw and attapulgite; the prepared hydrogel has a releasing effect for nitrogen and boron fertilizer. Liu *et al.* [23] synthesized superabsorbent hydrogels by the graft polymerization between chemically modified wheat straw and AA by radical polymerization. Liu *et al.* [22] used wheat straw, AA, and poly(vinyl alcohol) to synthesize cellulose-grafted poly acrylic potassium/poly vinyl alcohol semi-interpenetrating network hydrogels. El-Saied *et al.* [25] synthesized environment-friendly and low-cost hydrogels from straw. Currently, rice and wheat straws are the main straws used to produce superabsorbent hydrogels. Wan *et al.* [17] prepared superabsorbent hydrogels by the graft copolymerization between the corn straw, AA, AM, and 4-styrene sodium sulfate. Nevertheless, the hydrogels exhibited high-temperature resistance and salt resistance.

2-Acrylamido-2-methylpropanesulfonic acid (AMPS) is a multigroup anionic amide monomer. Its strong anionic nature, solubility, and good salt resistance result from the presence of sulfonic groups. It has better stability towards hydrolysis and acid/base resistance, and thermal stability because of the steric effect [26]. In particular, the AMPS products are inexpensive and therefore have become more significant in the superabsorbent field. If corn straws can be used to synthesize superabsorbent hydrogels with AMPS, not only “trash to treasure” can be achieved, but also the high-temperature and salt resistances can be realized. In this study, corn straws were used as the raw material; straw cellulose-AMPS-AA superabsorbent hydrogel was prepared by the radical graft copolymerization of straw cellulose, AMPS, and AA. The microstructure, thermal stability, rheology, salt resistance, and water retention ability of the as-prepared hydrogels were studied.

2. Materials and Methods

2.1. Materials

Analytical reagent grade sodium hydroxide, hydrogen peroxide, ethanol, acrylic acid (AA), *N,N'*-methylenebisacrylamide (MBA), 2-acrylamido-2-methylpropanesulfonic acid (AMPS), and potassium persulfate (KPS) were supplied by Tianjin Fuchen Chemicals (Tianjin, China). Corn straws were purchased from Huji factory, Huimin, Binzhou, China.

2.2. Preparation of Sulfonic Cellulose by Pretreating Corn Straws

Dry corn straws were ground and sieved using a 40-mesh sieve. Then, the resulting corn straw crash was made alkaline with 15% NaOH solution at 55 °C in a water bath for 2.5 h. The resulting solution was oxidized and bleached by H₂O₂, dried, and ground to get cellulose. The obtained cellulose was immersed in 17.5% NaOH solution and stirred for 1 h, followed by immersing in deionized water for 3 h, washed and neutralized with deionized water, filtered, and dried to afford alkaline fibers. The resulting alkaline fibers (1.6 g) and 100 mL deionized water were added to a

250 mL three-neck flask. The resulting mixture was stirred for 10 min at 40 °C under N₂, followed by adding KPS. After 20 min, 4.8 g AMPS monomer was added. After another 4 h, the sulphonated cellulose was cooled, washed successively with water and ethanol, and dried.

2.3. Synthesis of Superabsorbent Hydrogels

The as-prepared sulfonated cellulose (1 g) was dissolved in 10 mL water at 80 °C under N₂. After pasting for 10 min, the mixture was cooled in the temperature range 40–60 °C. KPS was added to the resulting mixture, followed by adding a certain amount of AA neutralized by NaOH. After a while, MBA was added until the hydrogels were produced. In addition, a control hydrogel sample was synthesized from AA without adding the sulfonated cellulose. The formulation for the control sample is listed in Table 1. The resulting hydrogels were dried at 80 °C in an oven for 24 h and then ground. The dried product was milled and screened for a particle size of 100 mesh.

Table 1. Formulations and process parameters of superabsorbent hydrogels.

Number	Pretreated straw (g)	AA (g)	MBA/AA (%)	KPS/AA (%)	Neutralization value (%)	Temperature (°C)
SH-0	0	6	0.8	1.5	70	40
SH-1	0	6	0.4	1.5	70	40
SH-2	1	6	0.8	1.5	70	40
SH-3	1	6	1.2	1.5	70	40
SH-4	1	6	1.6	1.5	70	40
SH-5	1	6	2.0	1.5	70	40
SH-6	1	6	2.4	1.5	70	40
SH-7	1	4	0.8	1.5	70	40
SH-8	1	5	0.8	1.5	70	40
SH-9	1	7	0.8	1.5	70	40
SH-10	1	8	0.8	1.5	70	40
SH-11	1	9	0.8	1.5	70	40
SH-12	1	6	0.8	1.0	70	40
SH-13	1	6	0.8	2.0	70	40
SH-14	1	6	0.8	2.5	70	40
SH-15	1	6	0.8	3.0	70	40
SH-16	1	6	0.8	3.5	70	40
SH-17	1	6	0.8	1.5	30	40
SH-18	1	6	0.8	1.5	40	40
SH-19	1	6	0.8	1.5	50	40
SH-20	1	6	0.8	1.5	60	40
SH-21	1	6	0.8	1.5	80	40
SH-22	1	6	0.8	1.5	70	35
SH-23	1	6	0.8	1.5	70	45
SH-24	1	6	0.8	1.5	70	50
SH-25	1	6	0.8	1.5	70	55
SH-26	1	6	0.8	1.5	70	60

AA, acrylic acid; MBA, *N,N'*-methylenebisacrylamide ; KPS, potassium persulfate.

2.4. Characterization of Hydrogels

2.4.1. Measurement of Swelling Ratio *Q*

After sieving the dried hydrogels using a 40-mesh sieve, a certain amount of the sample was transferred to a tea bag (100 mesh, 10 × 12 cm²) and then immersed in deionized water for 48 h at room temperature. After the swelling equilibrium was achieved, the samples were weighed.

The swelling ratio (*Q*) was calculated by using the following formula.

$$Q = (W_1 - W_0)/W_0 \quad (1)$$

where *W*₀ and *W*₁ are the mass of the dry and swollen hydrogels, respectively.

2.4.2. Fourier Transform Infrared Spectroscopy (FTIR) Analysis of Hydrogels

The corn straws, pretreated corn straws, and hydrogels were ground into fine powders, mixed with KBr, and pressed into pellets for FTIR analysis. FTIR spectra were scanned in the wavelength range 400–4000 cm^{-1} .

2.4.3. Measuring the Swelling Dynamics of Hydrogels

A certain amount of hydrogels (a particle size of 100 mesh) was transferred to a tea bag. Then, the tea bag was immersed into deionized water, until constant mass of achieved.

2.4.4. Salt Resistance of Hydrogels

NaCl, CaCl_2 , and AlCl_3 solutions with different concentrations were prepared (NaCl, CaCl_2 , and AlCl_3 can be completely dissociated at different concentrations). The dry hydrogel samples with the same mass were immersed in salt solutions. Salt resistance was determined by the swelling ratio when the hydrogel sample reached saturated absorption in salt solutions at different concentrations.

2.4.5. Microstructure Analysis of Hydrogels

The hydrogels were freeze-dried (pre-freeze-dried at $-40\text{ }^\circ\text{C}$ for 48 h under atmospheric pressure, then freeze-dried at $-70\text{ }^\circ\text{C}$ for 48 h, followed by freeze-drying for another 48 h at 10 Pa in a vacuum frozen dryer. The surface of the hydrogel sample was coated with Au. The microstructure of the hydrogel sample was measured using a Quanta 250 SEM (FEI Company, Hillsboro, OR, USA).

2.4.6. X-ray Diffraction (XRD) Characterization of the Composite Hydrogel

The freeze-dried hydrogel sample was ground into a fine powder. Diffraction pattern of the dried powder was obtained using an X-ray diffractometer (Rigaku DMAX-2000, Rigaku industrial corporation, Osaka, Japan), equipped with a copper target ray.

2.4.7. Thermal Gravity Analysis (TG)/Differential Thermal Gravity (DTG) Analysis of Hydrogels

The dried hydrogels (8–10 mg) were analyzed using an STA409C131F thermogravimetric analysis (TGA, NETZSCH Company, Bavarian State, Germany) in the temperature range 30–600 $^\circ\text{C}$ at a heating rate of 5 $^\circ\text{C}/\text{min}$.

2.4.8. Water Retaining Analysis

The hydrogels (8–10 mg) were analyzed by TGA in the temperature range 25–150 $^\circ\text{C}$ at a heating rate of 3 $^\circ\text{C}/\text{min}$. The residual masses of the hydrogels were recorded at different temperatures.

2.4.9. Water Reabsorption of Hydrogels

A certain amount of hydrogels was swollen in distilled water to reach the equilibrium. The saturated hydrogels were dried at 90 $^\circ\text{C}$ to a constant weight. The dried hydrogels were reimmersed into deionized water until equilibrium was established. The “swell-dry-swell again” process was repeated multiple times. In this study, the recyclability ratio (r) was proposed as the index to describe the water reabsorption, where r is the swelling ratio after n times of drying/initial swelling ratio.

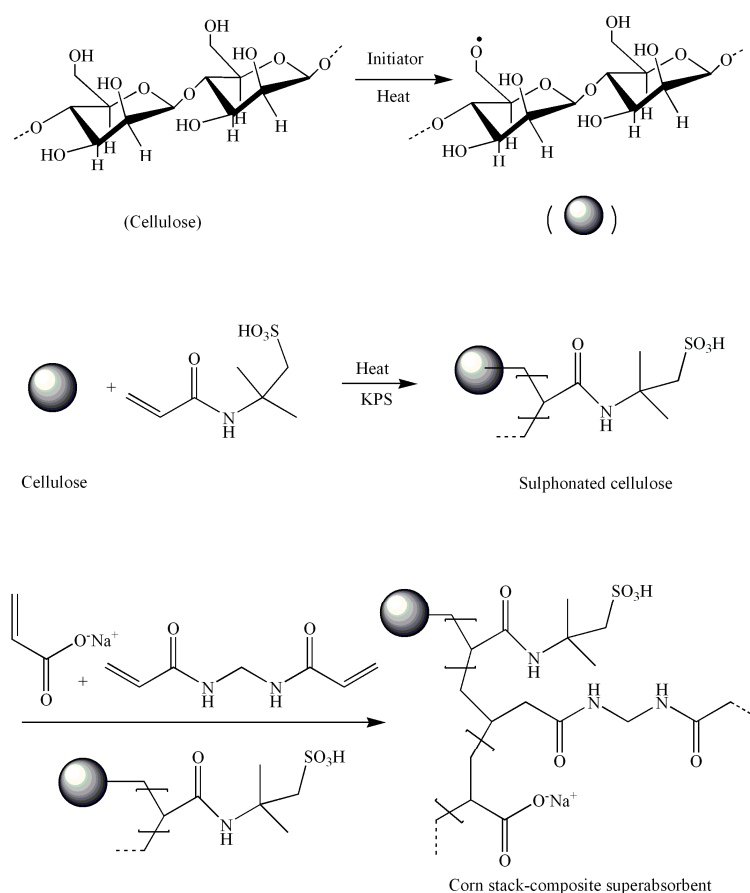
2.4.10. Rheological Properties of Hydrogels

The saturated hydrogels were analyzed using a rheology meter (Anton Paar, Ashland, VA, USA, PhysicalMCR302). The storage modulus was measured using a 50 mm parallel clamp at a slit width of 0.5 mm, strain 2%, and frequency 0.1 Hz [27].

3. Results and Discussion

3.1. FTIR Analysis

The initiator KPS can decompose to sulfates and sulfite radicals under heating. These free radicals attack the hydroxyl groups on the cellulose polysaccharides substrates. The cellulose polyacyloxy free radicals were produced by hydrogen abstraction. These macromolecular free radicals can initiate the grafting reaction of AMPS/AA onto the backbone of corn straw cellulose. The polymer chains formed a 3D network upon crosslinking with MBA. Scheme 1 illustrates the mechanism of the graft copolymerization. FTIR spectroscopy was used to determine the functional groups of the composite hydrogels.



Scheme 1. Proposed preparation mechanism for corn straw-co-AMPS-co-AA hydrogel.

Figure 1 shows the FTIR spectra of the corn straw before and after the pretreatment. The broad peak at 3409 cm^{-1} was attributed to the $-\text{OH}$ stretching vibration in lignin, cellulose, and hemicellulose molecules. The stretching vibrations of the $\text{C}-\text{H}$ bonds of $-\text{CH}_2$ moiety in cellulose and hemicellulose molecules were observed at 2922 cm^{-1} . The peak at 1731 cm^{-1} corresponded to the stretching vibration peak of nonconjugated carbonyl groups in lignin molecules. The peaks at 1640 and 1401 cm^{-1} were attributed to the stretching vibration of the $\text{C}=\text{C}$ backbone of the aromatic rings. The peak at 1060 cm^{-1} was attributed to the stretching vibration of the glycosidic bonds on cellulose and hemicellulose, confirming that the corn straw contains a significant amount of lignin, cellulose, and hemicellulose. After the pretreatment, the intensities of the peaks at 3409 and 1731 cm^{-1} decreased, indicating that lignin was modified by the pretreatment. The $-\text{OH}$ stretching peak at 3409 cm^{-1} became wide; the stretching peak of the $\text{C}-\text{H}$ group in $-\text{CH}_2$ at 2922 cm^{-1} decreased; the

stretching peak of S=O in the sulfonic acid groups appeared at 1139 cm^{-1} ; and the stretching peak of newly formed functional carboxyl functional group was observed at 1128 cm^{-1} . The FTIR analysis confirmed that AMPS was successfully grafted onto the treated corn straws.

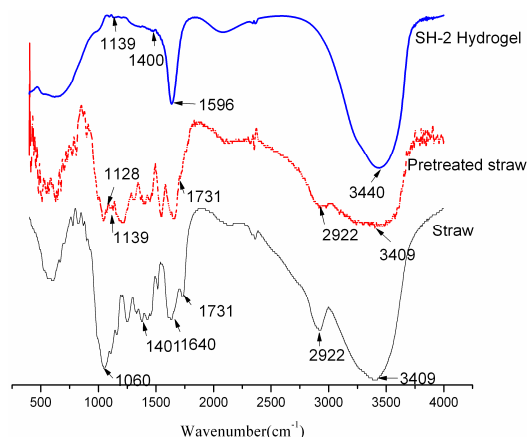


Figure 1. FTIR of straw, pretreated straw and hydrogel.

As shown in the FTIR spectrum of the superabsorbent hydrogel corn straw-co-AMPS-co-AA (Figure 1), the stretching vibration peaks of the –OH group of cellulose and the S=O group of sulfonic acid groups appeared at 3440 and 1139 cm^{-1} , respectively. The stretching vibration peaks at 1440 and 1596 cm^{-1} were attributed to the C=C backbone of the aromatic rings and –COO– groups, respectively. All these peaks verified that AA was successfully grafted onto the pretreated corn straws.

3.2. XRD Characterization

The XRD patterns of the corn straw, pretreated corn straw, and composite hydrogels are shown in Figure 2. Two obvious diffraction peaks were observed in the XRD pattern of corn straw, indicating that corn straws had a polycrystalline structure. However, the intensity and range of the diffraction peaks of the pretreated corn straw (pretreated by NaOH and H₂O₂) significantly decreased, indicating that after bleaching by H₂O₂, the hydrogen bonds in the crystalline regions of the straw cellulose chains were broken, thus decreasing the degree of crystallinity. The sharp diffraction peaks of the superabsorbent hydrogel disappeared and larger and wider diffusion peak appeared within in a wider range, indicating that the crystallized structure of the corn straw transformed into an amorphous structure, because the grafting reaction between the corn straw and monomers changed the original aggregation state of the corn straw and completely destroyed the crystalline structure. Therefore, the synthesized corn straw hydrogels had a noncrystalline structure.

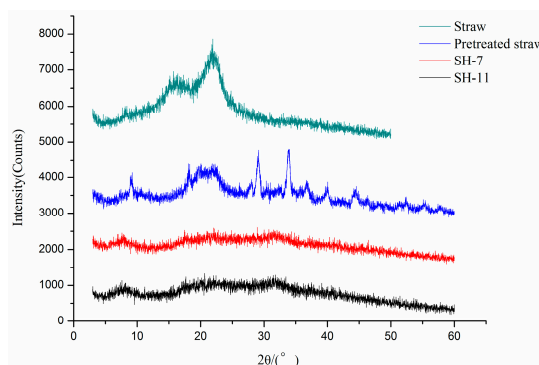


Figure 2. XRD of straw, pretreated straw and hydrogels.

3.3. Effect of MBA on Q Value Of Hydrogel

Figure 3a shows the variation in the Q values of the hydrogels with MAA content. When the amount of crosslinker was <1.2%, the Q of the hydrogels increased with increasing content of crosslinker. When the crosslinker was >1.2%, the Q of hydrogel decreased with increasing content of crosslinker, because no network structure was formed at a low concentration of crosslinker. Water could be only absorbed by the hydrophilic groups on the surface of the hydrogels, thus the Q value remained low. Nevertheless, very high concentration of crosslinker would result in excessively high crosslinking and smaller voids in the network, thus decreasing the Q value [23].

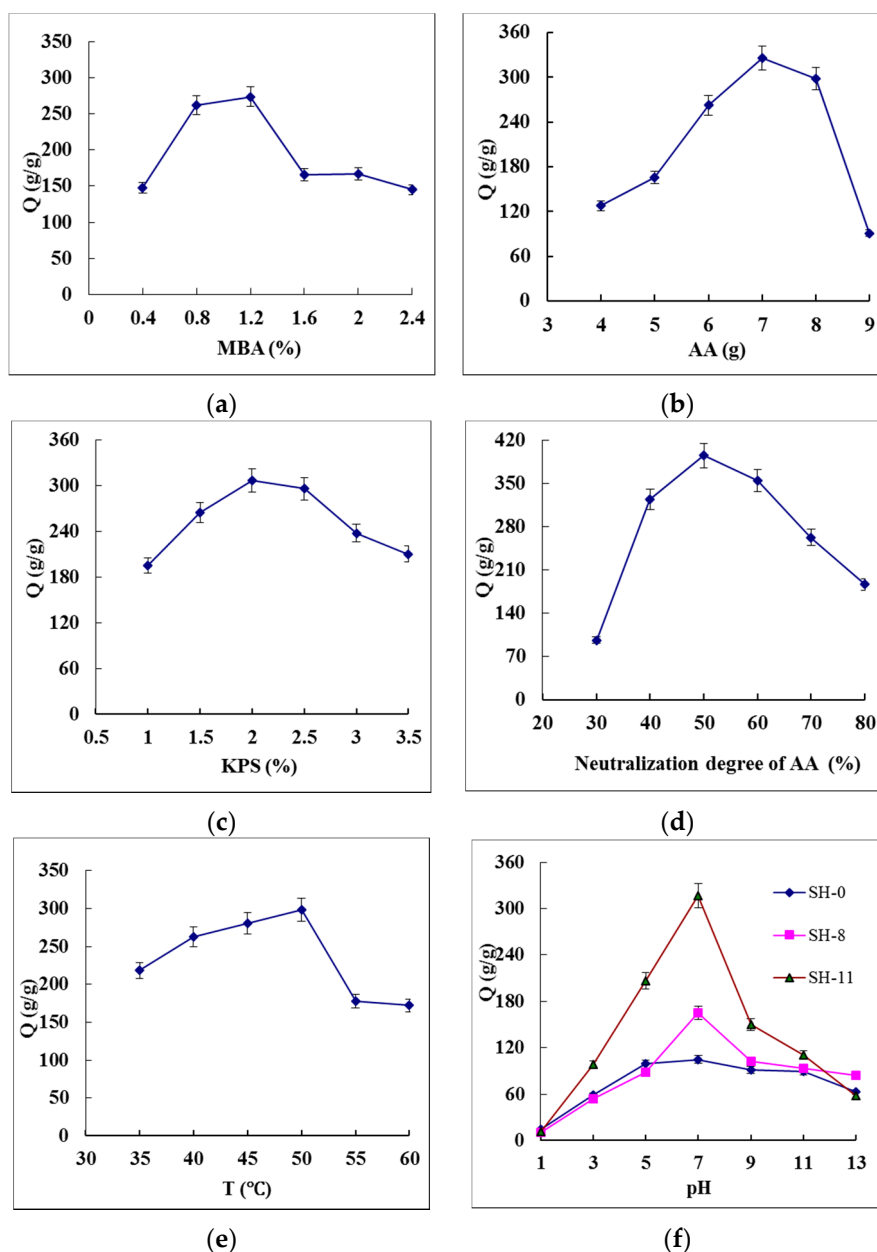


Figure 3. Effect of MBA (a), AA (b); KPS (c); neutralization degree of AA (d); temperature (e); and pH values (f) on water absorbency of hydrogels.

3.4. Effect of AA Content on the Swelling Ratio of Hydrogel

Figure 3b shows the effect of AA on the Q value of the hydrogel. With increasing concentration of AA, the Q values of the hydrogels increased and then decreased. When AA amount was >7 g, the Q values of the hydrogels decreased, because at higher AA concentrations, the collision probability between monomers would increase, thus increasing the graft length of the sulfonated cellulose, favoring the formation of a polymeric network at higher Q values of the hydrogels. High AA concentrations would lead to self-polymerization and lower swelling ratio. The optimum ratio between the sulfonated cellulose and monomer was determined as 1:7.

3.5. Effect of KPS on the Swelling Ratio of Hydrogel

Figure 3c shows the effect of KPS on the Q value of hydrogel. The Q values of the hydrogels increased, followed by a decrease with increasing amounts of KPS. The maximum Q value was observed at 2% KPS, because the polymerization was initiated by the free radicals generated from KPS under heat. More initiators would produce more free radicals that can enhance the grafting efficiency. Therefore, the hydrogel formation was enhanced, thus increasing the Q value. However, too much initiator would produce too many free radicals, thus increasing the collision probability between free radicals, eventually terminating the reaction [13]. The generated short graft chains would not form a 3D network easily, thus decreasing the Q value.

3.6. The Effect of Neutralization Degree of AA on Swelling Ratio

Figure 3d shows the effect of neutralization degree of AA on the Q value. When neutralization degree was $<50\%$, the Q value of the hydrogels increased with increasing degree of neutralization. When the degree of neutralization was $>50\%$, the Q values of the hydrogels gradually decreased, relative to the polymerization activity of AA. At a low degree of neutralization, the grafting reaction was too fast to control, thus easily forming a high-density polymer. In the meantime, AA molecules were self-polymerized and highly crosslinked, thus decreasing the Q values. With increasing degree of neutralization, the concentration of AA decreased and the concentration of hydrophilic sodium acrylate ($-\text{COONa}$) increased, thus increasing the swelling ratio. The electrostatic repulsion among the COO^- groups can expand the network of the hydrogels and decrease the reaction rate, favoring higher Q s [16]. When the degree of neutralization was $>50\%$, the activity of AA monomers decreased, thus the reaction rate decreased and solubility increased, decreasing the Q s.

3.7. Effect of Temperature on Swelling Ratio of Hydrogel

Figure 3e shows the effect of temperature on the Q values of hydrogels after the pasting reaction. The Q values increased and then decreased with increasing temperature, and reached to the maximum at 50°C . Less free radicals could be produced at such a low temperature, and thus may decrease the rate of grafting reaction, resulting in low Q s. With increasing temperature, more free radicals could be produced and the monomer reactivity may increase; therefore, the grafting and chain growth rate increased [16], thereby increasing the Q values of the hydrogels. When the temperature was $>50^\circ\text{C}$, the excessive free radicals generated from the decomposition of initiator increased the reaction rate, thus decreased the grafting molecular weight and were partly crosslinked, forming a less efficient network structure. All these decreased the Q s.

3.8. Effect of pH on Swelling Ratios of Hydrogels

Figure 3f shows the effect of pH on the Q values of the hydrogels, indicating that the Q values of the hydrogels were sensitive to pH. When pH was <7 , the Q value increased with increasing pH. The protonation of most of the carboxyl acid groups resulted in weaker repulsion between anions, thus decreasing Q s of the hydrogels. When pH was increased to seven, some carboxyl acid groups dissociated, and the Q could be higher, because of the electrostatic repulsion between the carboxyl

acid groups. When pH was >8, the Q value decreased with increasing pH, because the Na^+ cations from NaOH shield the $-\text{COO}^-$ groups and prevent the anion–anion repulsion [16]. The swelling ratios of SH-8 and SH-11 hydrogels were higher than that of the control hydrogel SH-0, because the pretreatment of corn straws increased the amount of hydroxyl and sulfonic acid groups. The water absorption was probably enhanced by the repulsion between the negatively charged groups.

3.9. Effect of Salt Solution on the Swelling Ratio of Hydrogel

Figure 4 shows the Q values of the hydrogels in different salt solutions. The Q values of the hydrogels increased with increasing concentration of salt solution, especially within the concentration in the range 0–0.05 M. Comparing the three salt solutions, the order of the Q values is as follows: $\text{NaCl} > \text{CaCl}_2 > \text{AlCl}_3$. Based on the Flory equation, the Q would be lower at higher ion concentrations and decreased because of decreasing ion concentration difference between the concentration of dissociated ions inside the hydrogels and ion concentration in the solution [28]. Higher-covalent cations would aggregate the hydrogels and decrease the swelling degree, thus increasing the internal crosslinking degree and significantly decreasing the Q values of the hydrogels in salt solutions. The higher the covalence, the more significant effect on the Q value [16].

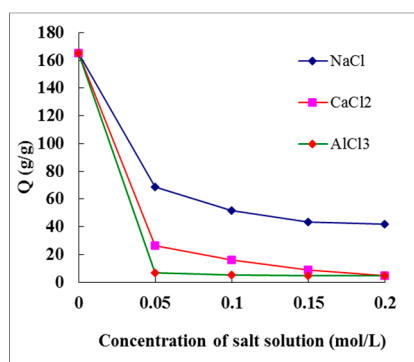


Figure 4. Water absorbency of hydrogels in salt solutions.

3.10. Swelling Dynamics of Hydrogels

Figure 5 shows the dynamic curves of several hydrogels. In the first 15 min, the swelling ratio of the hydrogels increased fast. After 15 min, the increasing rate decreased, and the swelling achieved equilibrium at ~20 min. Compared to the control hydrogel (SH-0), the swelling ratios and swelling rates of SH-2 hydrogel (25% pretreated corn straw) and SH-9 hydrogel (14% pretreated corn straw) both increased. With more corn straw, there would be more grafting g points, favoring the grafting reaction, forming a 3D network, thus increasing the water absorptivity. However, the swelling rate and ratio of SH-9 (14% pretreated straw) were higher than those of SH-2 (25% pretreated straw), indicating that the increased amount of corn straw may not result in better water absorptivity of hydrogels, because besides cellulose, corn straw contains a lot of lignin and hemicellulose. The phenol units in lignin can inhibit the polymerization, indicating that too excess corn straws would make the grafting reaction difficult and thus inhibit the formation of a 3D network. The swelling dynamics of the hydrogels agreed with the following exponential variation equation [29,30].

$$S_t = S_c(1 - e^{-t/\tau}) \quad (2)$$

where S_t (g/g) is the swelling ratio of hydrogels at t (s), S_c (g/g) is the swelling ratio at equilibrium, t (s) is the absorption time, and τ (s) is the time required to reach 40% of the maximum swelling ratio. The t values of SH-0, SH-7, and SH-9 hydrogels were 87.4, 90.2 and 120.3 s, respectively.

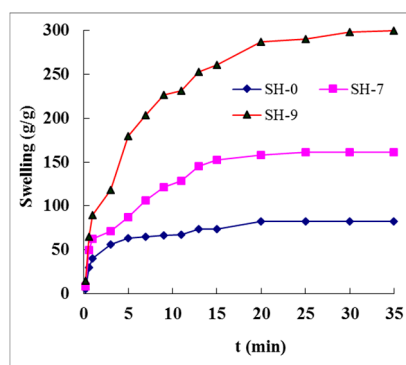


Figure 5. Swelling kinetics curves of different hydrogels.

3.11. Microstructure Analysis of Hydrogels

Figure 6a,b shows the SEM micrographs of the corn straw before and after the modification. Figure 6a shows that the parallel fibers compacted and ordered into a fiber bundle. The micropores were closed and many reactive hydroxyls were sealed. Figure 6b shows that after the pretreatment by NaOH and H₂O₂, the surface morphology of the corn straw significantly changed. The fiber structure became loose; the specific surface area of cellulose increased; some micropores were observed on the fiber extension surface, thus decreasing the degree of crystallinity. All these factors enhanced the surface wettability of cellulose to reagent and improved its reactivity.

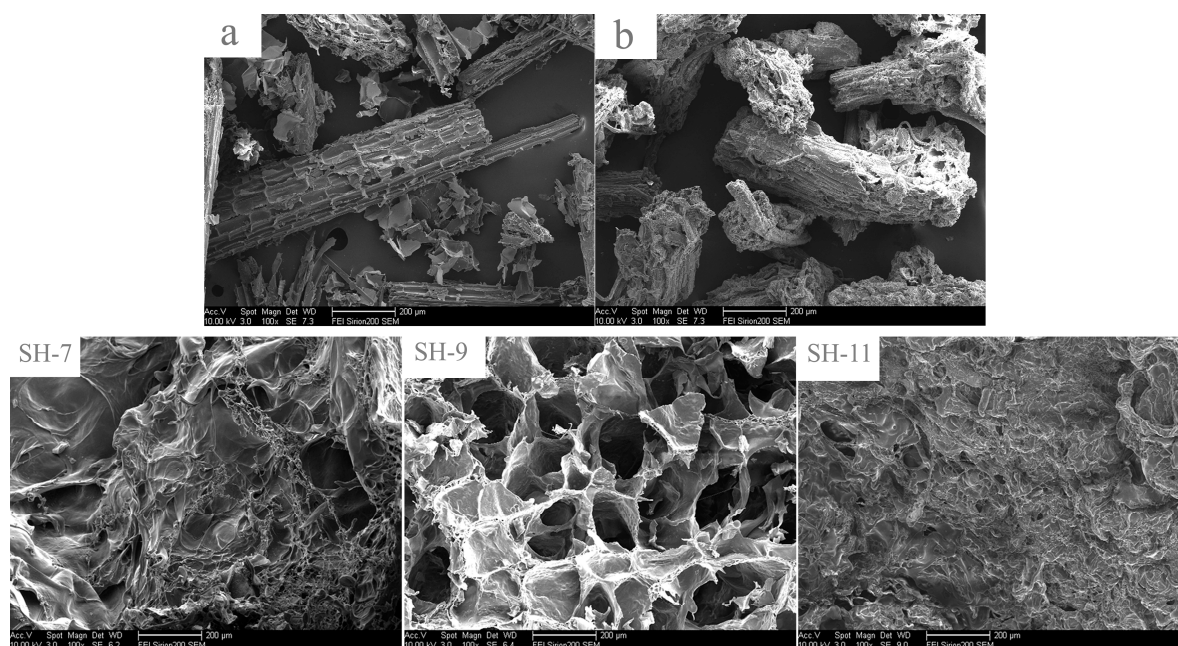


Figure 6. SEM micrographs of straw (a), pretreated straw (b), and hydrogels (SH-7, SH-9, SH-11).

Figure 6 (SH-7, SH-9, and SH-11) shows the microstructure of the freeze-dried corn straw-co-AMPS-co-AA hydrogels. No regular fiber tissue was observed on the surface, confirming that cellulose reacted with AMPS and AA to form a 3D network. The surface of the hydrogels corrugated and filled with micropores and capillaries. These structures were helpful to improve the water absorptivity of the hydrogels. The surface morphologies of three different hydrogels were significantly different. The surface of SH-7 hydrogel (20% pretreated straw) was the most corrugated and filled with some micropores. The surface of SH-9 hydrogel (13% pretreated straw) was full of

evenly distributed large pores, whereas the surface of SH-11 hydrogel (10% pretreated straw) was moderately corrugated and filled with a few micropores. The size of the micropores of the hydrogels is as follows: SH-9 > SH-7 > SH-11, and this is in accordance with the swelling ratio results.

3.12. Thermal Stability

The TG curves of the superabsorbent composites are shown in Figure 7, exhibiting three degradation steps. At the first stage (<140 °C), the weight loss occurs because of the evolution of absorbent and bound water in the network of hydrogels. The second stage (from 203–405 °C) is because of the dehydration of the carbohydrate chains and breaking of the C–O–C glycosidic bond of the cellulose chain. The third stage shows a sharp weight loss in the temperature range 415–490 °C, because of the oxidation of charred product. SH-2 and SH-7 hydrogels showed obvious differences in higher temperature range. The thermal decomposition for SH-2 hydrogel consists of the following stages: first 19.2% weight loss in the temperature range 203–405 °C and another 24.9% weight loss in the range 415–490 °C. Similarly, SH-7 first lost 18.6% weight from 203 to 405 °C and then lost 21.3% weight from 415 to 490 °C. The result indicate that SH-7 is more thermally stable, perhaps because of the fact that the cellulose chain has a higher thermal stability as compared to the carbohydrate chains, and thus enhanced the overall thermal stability of SH-7 hydrogel.

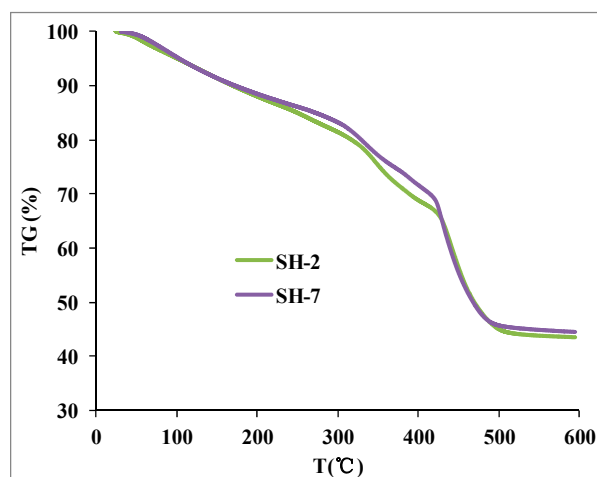


Figure 7. TGA curves of SH-2 and SH-7 hydrogels.

3.13. Storage Modulus Analysis of Hydrogels

Figure 8 shows the storage modulus of different hydrogels with different angular frequencies. The storage moduli of the hydrogels increased gradually with increasing angular frequency. At the same angular frequency, the storage modulus increased and then decreased with increasing amount of AA. When the amount of AA was 7 g, SH-9 hydrogel showed the maximum storage modulus, because more AA would increase the length of polymer, and the electrostatic repulsion could expand the 3D network of the hydrogels, enhancing the toughness of polymer and strength of the hydrogels. When AA was >8 g, the storage moduli of the hydrogels decreased, probably because of weaker hydrogen bonds between the carboxyl and amide groups [17].

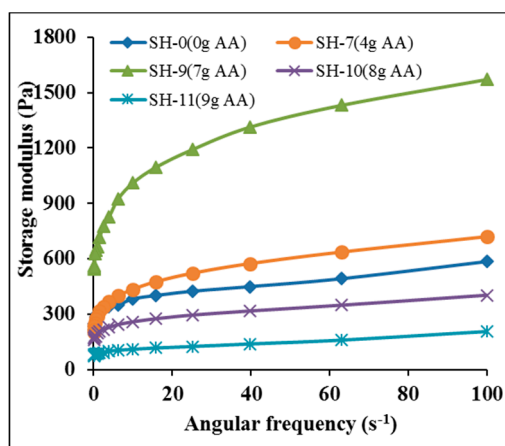


Figure 8. Storage modulus of hydrogels.

3.14. Water Retainability

Figure 9 shows the water retainability curves of the hydrogels with increasing temperature. The water retainability of the straw and the composite hydrogel increased with increasing amount of the pretreated corn straw. When the corn straw content was 25%, the highest water retainability was observed for SH-7 hydrogel. The value remained 68% at 80 °C. At higher corn straw content, more crosslinking favored the grafting reaction, resulting in a better 3D network, thus effectively increasing the retainability of water molecules. In contrast, the pretreated straw (sulfonated cellulose) contains hydrophilic functional groups such as carboxyl and amide groups, and carboxylate and sulfonate anions. During the absorption, the carboxylate and sulfonate anions dissociated, leading to electrostatic repulsion and the expansion of the carbon backbone. Meanwhile, the hydrophilic carboxyl and amide would interact with water molecules through hydrogen bonds, forming a network structure, thus water molecules will be difficult to diffuse from the saturated corn straw hydrogels at certain temperatures.

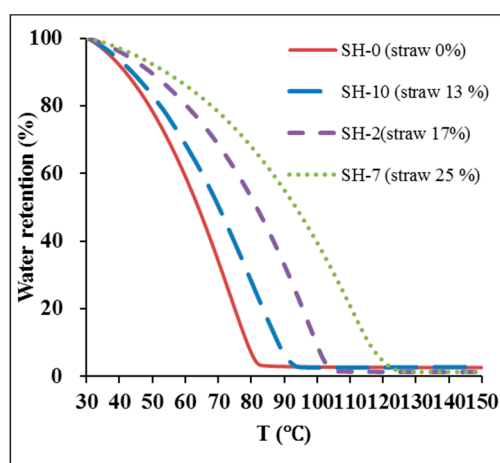


Figure 9. Water retention curve of hydrogels.

3.15. Recyclability of Hydrogels

Table 2 shows the swelling ratio after “swell-dry-swell” process. After five times water absorption or salt absorption, the swelling ratio decreased slightly, but was still high. The swelling ratio of SH-2 and SH-9 were 196 g/g with an r value of 75% and 256 g/g with an r value of 78.5%,

respectively. These results indicate that the corn straw hydrogels could be recycled owing to their r values.

Table 2. The repetitive absorption of the hydrogel.

Number	Repeat number	1	2	3	4	5
SH-2	Water absorption (g/g)	263	270	251	219	196
	r	1	1.03	0.95	0.81	0.75
SH-9	Water absorption (g/g)	326	332	305	283	256
	r	1	1.02	0.94	0.87	0.81

4. Conclusions

Corn straws were chemically modified to sulfonated cellulose by the grafting copolymerization with AMPS. Then, the pretreated corn straws were graft polymerized with AA to prepare corn straw-*co*-AMPS-*co*-AA hydrogels. The FTIR results confirmed the grafting copolymerization between the corn straw and AMPS, and the pretreated corn straw and AA. The XRD results showed that the degree of crystallinity decreased during the pretreatment and graft copolymerization. Corn straw-*co*-AMPS-*co*-AA hydrogels has a noncrystalline structure. The SEM results showed that after the treatment with NaOH and H₂O₂, the surface of the corn straw became loose and filled with micropores, thus enhanced the reactivity of cellulose. The microstructure of corn straw-*co*-AMPS-*co*-AA showed that the surface of hydrogels was corrugated and full of micropores, thus favoring the water absorption. With a higher amount of corn straw, high-temperature water retainability of the composite straw hydrogel increased. The experimental results confirmed that the optimum water absorptivity of the corn straw hydrogels was achieved under the following conditions: crosslinker content of 1.2%, pretreated corn straw/monomer ratio, 1:7, initiator content, 2%; AA neutralization degree of 50%; and temperature, 50 °C. Moreover, the water reabsorption capability of corn straw-*co*-AMPS-*co*-AA hydrogels was very strong, and the hydrogels were efficiently recycled. We believe that the corn straw-*co*-AMPS-*co*-AA hydrogels have potential applications in the controlled delivery of bioactive agents in agriculture, construction, as well as fire extinguishing agents.

Acknowledgements: This study was supported by the National Natural Science Foundation of China (51304027); the project was funded by the China Postdoctoral Science Foundation (2014M560567 and 2015T80730), Shandong Province Science and Technology Development Plan Item (2014GSF120012), the State Key Program of Coal Joint Funds of National Natural Science Foundation of China (No.51134020, No.U1261205), and key technology projects for preventing major accident of National Security State Administration of Work Safety.

Author Contributions: Wei-Min Cheng and De-Ming Wang designed the research; Guo-Hua Liu contributed to the synthesis of corn straw-*co*-AMPS-*co*-AA hydrogels; Xiang-Ming Hu analyzed the data and wrote the paper.

Conflicts of Interest: The authors declare no conflict of interest.

References

- Juby, K.A.; Dwivedi, C.; Kumar, M.; Kota, S.; Misra, H.S.; Bajaj, P.N. Silver nanoparticle-loaded PVA/gum acacia hydrogel: Synthesis, characterization and antibacterial study. *Carbohydr. Polym.* **2012**, *89*, 906–913. [[CrossRef](#)] [[PubMed](#)]
- Vakili, M.R.; Rahneshein, N. Synthesis and characterization of novel stimuli-responsive hydrogels based on starch and L-aspartic acid. *Carbohydr. Polym.* **2013**, *98*, 1624–1630. [[CrossRef](#)] [[PubMed](#)]
- Wang, W.B.; Wang, A.Q. Nanocomposite of carboxymethyl cellulose and attapulgite as a novel pH-sensitive superabsorbent: Synthesis, characterization and properties. *Carbohydr. Polym.* **2010**, *82*, 83–91. [[CrossRef](#)]
- Ji, D.Y.; Kuo, T.F.; Wu, H.D.; Yang, J.C.; Lee, S.Y. A novel injectable chitosan/polyglutamate polyelectrolyte complex hydrogel with hydroxyapatite for soft-tissue augmentation. *Carbohydr. Polym.* **2012**, *89*, 1123–1130. [[CrossRef](#)] [[PubMed](#)]

5. Ji, Q.X.; Deng, J.; Xing, X.M.; Yuan, C.Q.; Yu, X.B.; Xu, Q.C.; Yue, J. Biocompatibility of a chitosan-based injectable thermosensitive hydrogel and its effects on dog periodontal tissue regeneration. *Carbohydr. Polym.* **2010**, *82*, 1153–1160. [[CrossRef](#)]
6. Zohuriaan-Mehr, M.J.; Omidian, H.; Doroudiani, S.; Kabiri, K. Advances in non-hygienic applications of superabsorbent hydrogel materials. *J. Mater. Sci.* **2010**, *45*, 5711–5712. [[CrossRef](#)]
7. Basta, A.H.; El-Saied, H.; El-Hadi, O.; El-Dewiny, C.Y. Evaluation of rice straw-based hydrogels for purification of wastewater. *Polym. Plast. Technol.* **2013**, *52*, 1074–1080. [[CrossRef](#)]
8. Jin, S.P.; Liu, M.Z.; Zhang, F.; Chen, S.L.; Niu, A.Z. Synthesis and characterization of pH-sensitivity semi-IPN hydrogel based on hydrogen bond between poly(*N*-vinylpyrrolidone) and poly(acrylic acid). *Polymer* **2006**, *47*, 1526–1532. [[CrossRef](#)]
9. Yu, J.; Pan, Y.P.; Lu, Q.F.; Yang, W.; Gao, J.Z.; Li, Y. Synthesis and swelling behaviors of P(AMPS-*co*-AAc) superabsorbent hydrogel produced by glow-discharge electrolysis plasma. *Plasma Chem. Plasma Process.* **2013**, *33*, 219–220. [[CrossRef](#)]
10. Blagodatskaya, E.V.; Ermolaev, A.M.; Myakshina, T.N. Ecological strategies of soil microbial communities under plants of meadow ecosystems. *Biol. Bull.* **2004**, *31*, 620–627. [[CrossRef](#)]
11. Chen, Y.; Tan, H. Cross-linked carboxymethylchitosan-*g*-poly(acrylic acid) copolymer as a novel super-absorbent polymer. *Carbohydr. Polym.* **2006**, *341*, 887–896. [[CrossRef](#)] [[PubMed](#)]
12. Zhang, J.; Li, A.; Wang, A. Synthesis and characterization of multifunctional poly(acrylic acid-*co*-acrylamide)/sodium humate super-absorbent composite. *React. Funct. Polym.* **2006**, *66*, 747–756. [[CrossRef](#)]
13. Zhang, J.; Wang, Q.; Wang, A. Synthesis and characterization of chitosan-*g*-poly(acrylic acid)/attapulgit super-absorbent composites. *Carbohydr. Polym.* **2007**, *68*, 367–374. [[CrossRef](#)]
14. Fekete, T.; Borsa, J.; Takács, E.; Wojnárovits, L. Synthesis of cellulose derivative based superabsorbent hydrogels by radiation induced crosslinking. *Cellulose* **2014**, *21*, 4157–4158. [[CrossRef](#)]
15. Yoshimura, T.; Matsuo, K.; Fujioka, R. Novel biodegradable superabsorbent hydrogels derived from cotton cellulose and succinic anhydride synthesis and characterization. *J. Appl. Polym. Sci.* **2006**, *99*, 3251–3256. [[CrossRef](#)]
16. Pourjavadi, A.; Samadi, M.; Ghasemzadeh, H. Fast-swelling superabsorbent hydrogels from poly(2-hydroxy ethyl acrylate-*co*-sodium acrylate) grafted on starch. *Starch Stärke* **2008**, *60*, 79–86. [[CrossRef](#)]
17. Wan, T.; Xiong, L. Synthesis and swelling properties of corn stalk-composite superabsorbent. *J. Appl. Polym. Sci.* **2013**, *130*, 698–703. [[CrossRef](#)]
18. Aloulou, F.; Boufi, S.; Labidi, J. Modified cellulose fibres for adsorption of organic compound in aqueous solution. *Sep. Purif. Technol.* **2006**, *52*, 332–342. [[CrossRef](#)]
19. Bertrand, I.; Prevot, M.; Chabbert, B. Soil decomposition of wheat internodes of different maturity stages: Relative impact of the soluble and structural fractions. *Bioresour. Technol.* **2009**, *100*, 155–163. [[CrossRef](#)] [[PubMed](#)]
20. Xie, L.H.; Liu, M.Z.; Ni, B.L.; Zhang, X.; Wang, Y.F. Slow-release nitrogen and boron fertilizer from a functional superabsorbent formulation based on wheat straw and attapulgit. *Chem. Eng. J.* **2011**, *167*, 342–348. [[CrossRef](#)]
21. Li, Q.; Ma, Z.H.; Yue, Q.Y. Synthesis, characterization and swelling behavior of superabsorbent wheat straw graft copolymers. *Bioresour. Technol.* **2012**, *118*, 204–209. [[CrossRef](#)] [[PubMed](#)]
22. Liu, J.; Li, Q.; Su, Y.; Yue, Q.Y.; Gao, B.Y. Characterization and swelling-deswelling properties of wheat straw cellulose based semi-IPNs hydrogel. *Carbohydr. Polym.* **2014**, *107*, 232–240. [[CrossRef](#)] [[PubMed](#)]
23. Liu, Z.X.; Miao, Y.G.; Wang, Z.Y.; Yin, G.G. Synthesis and characterization of a novel super-absorbent based on chemically modified pulverized wheat straw and acrylic acid. *Carbohydr. Polym.* **2009**, *77*, 131–135. [[CrossRef](#)]
24. Swantomo, D.; Rochmadi, R.; Basuki, K.T.; Sudiyo, R. Synthesis and characterization of graft copolymer rice straw cellulose-acrylamide hydrogels using gamma irradiation. *At. Indones.* **2013**, *39*, 57–64. [[CrossRef](#)]
25. El-Saied, H.; Basta, A.H.; Waly, A.I.; El-Hady, O.A.; El-Dewiny, C.Y.; Abo-Sedera, S.A. Evaluating the grafting approaches for utilizing the rice straw as environmental friendly and potential low cost hydrogels. *Emir. J. Food Agric.* **2013**, *25*, 211–224. [[CrossRef](#)]

26. Liu, Y.; Xie, J.J.; Zhu, M.F.; Zhang, X.Y. A study of the synthesis and properties of AM/AMPS copolymer as superabsorbent. *Polym. Mater. Sci. Eng.* **2004**, *289*, 1074–1078. [[CrossRef](#)]
27. Muniz, E.C.; Geuskens, G. Polyacrylamide hydrogels and semiinterpenetrating networks (IPNs) with poly(*N*-isopropylacrylamide): Mechanical properties by measure of compressive elastic modulus. *J. Mater. Sci. Mater. Med.* **2001**, *12*, 879–881. [[CrossRef](#)] [[PubMed](#)]
28. Castal, D.; Ricard, A.; Audebert, R. Swelling of anionic and cationic starch-based superabsorbents in water and saline solution. *J. Appl. Polym. Sci.* **1990**, *39*, 11–29. [[CrossRef](#)]
29. Omidian, H.; Hashemi, S.A.; Sammes, P.G.; Meldrum, I. A model for the swelling of superabsorbent polymers. *Polymer* **1998**, *39*, 6697–6704. [[CrossRef](#)]
30. Marandi, G.B.; Mahdavinia, G.R.; Ghafary, S. Collagen-g-poly(sodium acrylate-co-acrylamide)/sodium montmorillonite superabsorbent nanocomposites: Synthesis and swelling behavior. *J. Polym. Res.* **2011**, *18*, 1487–1499. [[CrossRef](#)]



© 2015 by the authors; licensee MDPI, Basel, Switzerland. This article is an open access article distributed under the terms and conditions of the Creative Commons by Attribution (CC-BY) license (<http://creativecommons.org/licenses/by/4.0/>).